

## Influence of a nonuniform thermal quench and circular polarized radiation on spontaneous current generation in superconducting rings

M. D. Croitoru<sup>1,2,6</sup>, B. Lounis<sup>3,4</sup> and A. I. Buzdin<sup>1,5</sup>

<sup>1</sup>University of Bordeaux, LOMA UMR-CNRS 5798, F-33405 Talence, France


<sup>2</sup>Departamento de Física, Universidade Federal de Pernambuco, 50670-901, Recife-PE, Brazil

<sup>3</sup>Université de Bordeaux, LP2N, F-33405 Talence, France

<sup>4</sup>Institut d'Optique & CNRS, LP2N, F-33405 Talence, France

<sup>5</sup>World-Class Research Center “Digital Biodesign and Personalized Healthcare”, Sechenov First Moscow State Medical University, Moscow 119991, Russia

<sup>6</sup>National Research University Higher School of Economics, Moscow 101000, Russia

 (Received 2 June 2021; revised 29 November 2021; accepted 4 January 2022; published 19 January 2022)

We theoretically study the nonequilibrium dynamics of the order parameter of a superconducting ring inhomogeneously quenched through its transition temperature. Numerical simulations based on spectral decomposition of the time-dependent Ginzburg-Landau equation reveal that current-carrying superconducting states can be generated in the ring under certain fast local temperature quench conditions. We also show that illumination of the ring with a circularly polarized electromagnetic radiation during rapid cooling strongly promotes the generation of current-carrying states with rotation directions controlled by the helicity of the radiation field.

DOI: [10.1103/PhysRevB.105.L020504](https://doi.org/10.1103/PhysRevB.105.L020504)

**Introduction.** Advances in the control and manipulation of macroscopic quantum systems now make it possible to study in detail the dynamics of phase transitions and the symmetry breaking processes that can result, such as those associated with the Kibble-Zurek mechanism (KZM) [1–4]. This mechanism explains the spontaneous generation of topological defects that occur in the order parameter of a system subjected to a rapid thermal quench leading to the spontaneous formation of Abrikosov vortices in superconductors. Indeed, when the thermal quenching time  $t_Q$  is shorter than the relaxation time of the system  $\tau_\Delta$ , the system is driven out of equilibrium and its symmetry is locally broken. This results in the formation of ordered regions with a typical size of about the correlation length  $\xi$ . The separate regions, whose relative phases are random, increase in size during the transition until they merge and eventually lead to the formation of vortices. The spontaneous generation of vortices upon rapid cooling has been demonstrated in superconducting films [5–8], heated by pulsed laser light above the critical temperature, and followed by a rapid cooling (rates  $>0.1$  K/ns), through the continuous phase transition. Magneto-optical images of vortices and antivortices randomly generated by KZM in niobium films have been reported [6,7].

An important step toward applications in vortex-controlled Josephson transport [9–11] is the development of a simple and scalable method to generate a vortex at any desired location of a superconducting electrode. The generation of single vortex pairs has been discovered upon local suppression of superconductivity caused by heating around a scanning tunneling microscope tip [12]. Recently, the on-demand optical generation of permanent single vortices at any desired position in a superconductor has been demonstrated. It is based on a

fast quench following the absorption of a tightly focused laser pulse that locally heats the superconductor above its critical temperature [13]. The experiment revealed *ex nihilo* creation of a single vortex pinned at the center of the hot spot with its counterpart opposite flux trapped tens of micrometers away at the superconductor boundaries.

In isolated superconducting rings, made of high-quality Nb films, Monaco *et al.* [14] studied the probability of single fluxoid generation over a wide range of parameters. They were able to vary the cooling rate over a range of more than four orders of magnitude and found that the probability clearly follows a scaling relation on the quenching time expected for the KZ mechanism. Previously thermally activated vortex states were observed by Kirtley *et al.* [15] in amorphous  $\text{Mo}_3\text{Si}$  rings when cooled through the normal-superconducting transition.

Recently, in order to explore new ways for the generation of light-stimulated magnetic states in superconducting systems [16], a theoretical description of the inverse Faraday effect (IFE) [17,18] in superconductors has been developed. It was experimentally demonstrated that illumination of the toroidal atomic Bose-Einstein condensate, an artificial superfluid system, by twisted light carrying a nonzero angular momentum produces dc persistent supercurrents [19,20]. Similar light-stimulated persistent currents can be expected in conventional solid-state superconductors [16].

In this Letter, we perform simulations based on time-dependent Ginzburg-Landau (TDGL) equations to show that the nonuniform cooling of a superconducting ring favors the generation of current-carrying superconducting states in the ring under certain fast local temperature quench conditions. We also show that in the case of uniform cooling, an illumination of the ring with a circularly polarized electromagnetic

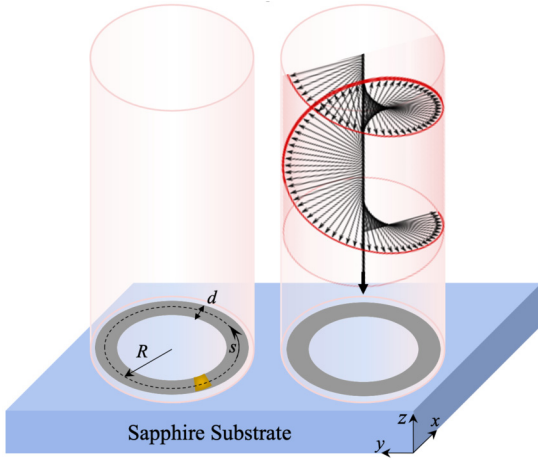


FIG. 1. Scheme of the thin superconducting ring on a substrate (top) nonuniformly cooled down after pulsed laser excitation; (bottom) uniformly cooled down after circularly polarized laser beam excitation. The yellow region at the ring corresponds to the hot/cold region at  $-s_0/2 < s < s_0/2$ .

radiation during a rapid quench strongly promotes the generation of current-carrying states through IFE with rotation directions controlled by the helicity of the radiation.

*Model and general settings.* We consider a planar superconducting ring having radius  $R$  (see Fig. 1), with width  $d$  and a thickness much smaller than the superconducting coherence length  $\xi(T)$  [21]. The ring is deposited on a thick transparent substrate with a very large heat capacity to ensure a high cooling rate.

We consider the situation when the ring is heated by a laser pulse up to the temperature  $T_{\text{heat}}$  above its critical temperature  $T_{c0}$ , and then starts to cool down rapidly to the substrate temperature  $T_0 < T_{c0}$ . Introducing  $\delta T = (T_{\text{heat}} - T_0)/T_{c0}$ , we can model the evolution of the ring temperature as

$$T^G(t) = T_0 + \delta T T_{c0} f(t/t_Q^G), \quad (1)$$

with  $f(x) = \exp(-x)$ , and  $t_Q^G$  the quenching time. We consider the situation where a small region of the ring  $-s_0/2 < s < s_0/2$  has more (less) effective heat contact with the substrate with a different local quench time  $t_Q^L$ . In this region

$$T^L(t) = T_0 + \delta T T_{c0} f(t/t_Q^L). \quad (2)$$

The situation  $t_Q^L < t_Q^G$  corresponds to a ‘‘cold point,’’ while  $t_Q^L > t_Q^G$  corresponds to a ‘‘hot point.’’ Assuming  $s_0 \ll \xi(T)$  [local region modeled by the  $\delta(\mathbf{r})$  function], we obtain for the temperature evolution

$$T(\theta, t) = T_0 + \delta T T_{c0} f(t/t_Q^G) + \delta(\theta) \frac{s_0}{R} \delta T T_{c0} [f(t/t_Q^L) - f(t/t_Q^G)], \quad (3)$$

where  $\theta$  is the polar angle related to the curvilinear coordinate  $s = R\theta$ . Note that the appearance of hot/cold points may occur occasionally or intentionally due to the nonhomogeneous thermal contact between the superconducting ring and substrate. For example, the presence/absence of the small oxide island on the substrate should play a role of a heat ascent/sink

with a different local quench time. A similar situation may be realized in samples with an inhomogeneous thickness and/or attached contacts. Point defects can also decrease the thermal conductivity and hence modify the thermal quench locally [22,23].

In the following we use the dimensionless coordinate  $s/\xi(0)$ , where  $\xi(0) = 0.85\sqrt{\xi_0 l}$  is the zero-temperature superconducting coherence length in the dirty limit ( $\xi_0 = \hbar v_F / 2\pi T_{c0}$ ) and  $l \ll \xi_0$  is the electron’s mean free path. The size of the region where the local quench is more (less) pronounced is characterized by the dimensionless parameter  $\gamma_0 \equiv s_0/\xi(0)$ .

To address the problem of fluctuation-driven nucleation and dynamics of the condensate we solve the stochastic time-dependent Ginzburg-Landau (sTDGL) equation of motion, which includes the Langevin term [24–26]. Assuming a ring radius smaller than the length of the relaxation of the electron-hole imbalance potential [24], we may eliminate the scalar potential from TDGL equations. We neglect the contribution to the magnetic field from the superconducting current, which is fully justified when the cross section of the ring-shaped superconductor is much smaller than the square of the London penetration depth  $\lambda^2(T_0)$ . Expressing the spatial coordinates in units of  $\xi(0)$ , the time in units of characteristic relaxation time  $\tau_\Delta = \pi \hbar / [8(T_{c0} - T_0)]$  at temperature  $T = T_0$ , and the vector potential  $\mathbf{A}(\mathbf{r}, t)$  in units of  $\Phi_0 / 2\pi \xi_0$ , one can write the sTDGL equation in the dimensionless form

$$\Gamma_\Delta \frac{\partial \Delta(\mathbf{r}, t)}{\partial t} = \frac{T_{c0} - T(\mathbf{r}, t)}{T_{c0} \epsilon_0} \Delta(\mathbf{r}, t) - |\Delta(\mathbf{r}, t)|^2 \Delta(\mathbf{r}, t) - \epsilon_0^{-1} (i\nabla + \mathbf{A})^2 \Delta(\mathbf{r}, t) + \zeta(\mathbf{r}, t). \quad (4)$$

Here,  $\epsilon_0 = 1 - T_0/T_{c0}$  and the complex relaxation time  $\Gamma_\Delta = 1 + i\eta$  takes into account a small imaginary part  $\eta$  arising from an electron-hole asymmetry [24,27–29]. The stochastic force  $\zeta(\mathbf{r}, t)$  describes the Gaussian random field of thermal fluctuations with ‘‘white-noise’’ correlations [30,31].

Considering the ring-shaped geometry described by the angle  $\theta = s/R$ , we may write the order parameter as

$$\Delta(\theta, t) = \sum_{n=-N_c}^{N_c} \psi_n(t) e^{-in\theta}. \quad (5)$$

The sTDGL transforms into a system of coupled differential equations for modes  $\psi_n(t)$ ,

$$\Gamma_\Delta \frac{\partial \psi_n(t)}{\partial t} = \left[ 1 - \frac{T^G(t) - T_0}{T_{c0} \epsilon_0} - \frac{1}{\epsilon_0 R^2} n^2 \right] \psi_n(t) - \sum_{l,m} \{\psi_l(t) \psi_m^*(t)\} \psi_{n+m-l}(t) - \frac{\gamma(t)}{T_{c0} \epsilon_0} \sum_n \psi_n(t) + \zeta_n(t), \quad (6)$$

where  $N_c$  sets a maximum number of modes we retain in our numerical calculations,  $\gamma(t) = \gamma_0 \delta T T_{c0} [f(t/\tau_Q^L) - f(t/\tau_Q^G)]/R$ , and  $\zeta_n(t)$  is the spectral representation of the noise term. We use the dimensionless local and global quench times,  $\tau_Q^G \equiv t_Q^G/\tau_\Delta$  and  $\tau_Q^L \equiv t_Q^L/\tau_\Delta$ , respectively. For

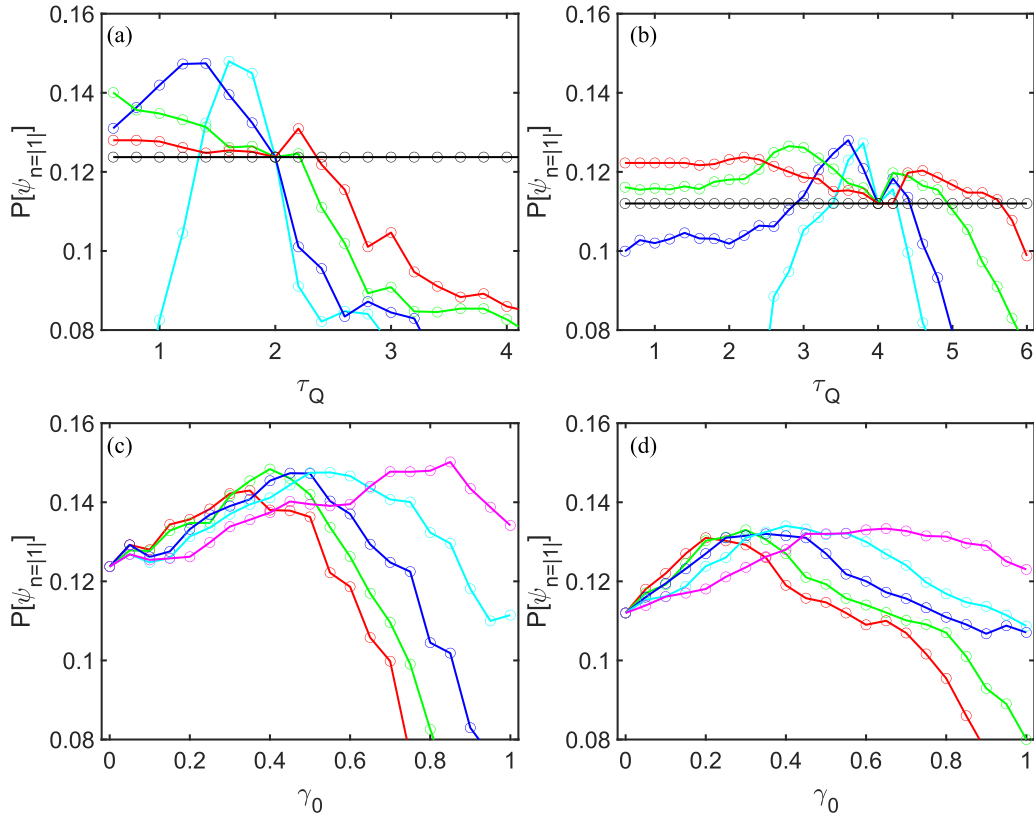


FIG. 2. State  $\psi_{n=|1|}$  generation probability as a function of local quench time  $\tau_Q^L$  for (a)  $\tau_Q^G = 2$  and (b) 4. The probabilities are presented for local quenching strengths  $\gamma_0 = 0$  (black),  $\gamma_0 = 0.1$  (red),  $\gamma_0 = 0.2$  (green),  $\gamma_0 = 0.5$  (blue), and  $\gamma_0 = 0.8$  (cyan). (c) State  $\psi_{n=|1|}$  generation probability as a function of quenching parameter  $\gamma_0$  for  $\tau_Q^G = 2$ . The probabilities are simulated for  $\tau_Q^L = 0.8$  (red),  $\tau_Q^L = 1.0$  (green),  $\tau_Q^L = 1.2$  (blue),  $\tau_Q^L = 1.4$  (cyan), and  $\tau_Q^L = 1.6$  (magenta). (d) Same as (c) for  $\tau_Q^G = 4$  and  $\tau_Q^L = 2.8$  (red),  $\tau_Q^L = 3$  (green),  $\tau_Q^L = 3.2$  (blue),  $\tau_Q^L = 3.4$  (cyan), and  $\tau_Q^L = 3.6$  (magenta).

details of the derivation of the dimensionless stochastic force term, see the Supplemental Material [32] (see also Refs. [21,30,31,33–39] therein).

*The local quench effect.* We first concentrate on the KZM in the presence of a local quench and consider the real relaxation time  $\Gamma_\Delta = 1$ . Note that the presence of a small imaginary part in the relaxation time does not qualitatively change the obtained results, but simply decreases the probability of the current state generation. The initial state corresponds to the absence of superconductivity  $T_{\text{heat}} > T_{c0}$ . The final equilibrium (metastable) state at  $T = T_0$  is obtained by the integration Eq. (6) at  $t > 0$  with the temperature profile of (3). We simulate the dynamics of  $\psi_n(t)$  by integrating the spectral sTDGL equation numerically using a fifth-order adaptive step-size Cash-Karp Runge-Kutta algorithm for more than  $N_{\text{it}} = 500$  noise realizations. Various observables, such as the probability of the  $n$ th mode, can be obtained after averaging over  $N_{\text{it}}$  noise realizations to provide a reliable and meaningful statistical estimate.

In the simulation we use the following parameters: ring radius  $R = 9.45$ , reduced equilibrium temperature  $\epsilon_0 = 0.1$ , temperature rise  $\delta\tilde{T} = 2$ , size of the local quench  $0 \leq \gamma_0 \leq 1.0$ , and the characteristic times of the local and global quenches  $0 \leq \tau_Q^{L(G)} \leq 10$ . We compute individual stochastic trajectories up to  $t = 200$  (there are no observable changes for  $t \gtrsim 70$ ).

When the global temperature reduces below  $T_{c0}$ , a normal supercooled phase develops. This phase is unstable, and decays into one of the minima due to the noise  $\zeta_n(t)$  fluctuations. Then nucleation of superconductivity starts and leads to a single stable mode after the decay of all the other ones (see the Supplemental Material Fig. S1 [32]). The probability of the  $n$ th mode realization,  $P_n(\psi_n; \infty)$ , is obtained after a time evolution  $t = 200$ .

Figure 2 shows the probability to find the stationary final state  $n = |1|$ ,  $P_{|1|}(\psi_{|1|}; \infty)$  as a function of local cooling duration  $\tau_Q^L$  and local quench strength  $\gamma_0$ . The results presented in the figure correspond to two values of the global cooling quench durations [ $\tau_Q^G = 2$  (left panels) and  $\tau_Q^G = 4$  (right panels)]. One can clearly see that the probability of finding a final state with  $|n| = 1$  is rather large (up to 15%), while the probability of obtaining  $|n| > 1$  states is negligibly small. As expected, the calculations show that the probability of generating a fluxoid with  $n = +1$  is the same as that with  $n = -1$ . Therefore the figure displays only the joint probability, for  $|n| = 1$ . Clearly, an increase of the global quench time reduces the probability of  $n \neq 0$  state generation, in accordance with KZM.

One may see that the presence of a *cold* spot provides more favorable conditions for  $|n| = 1$  orbital state generation compared to a *hot* spot. In both cases the presence of a local quench can increase the probability of  $n = \pm 1$  state

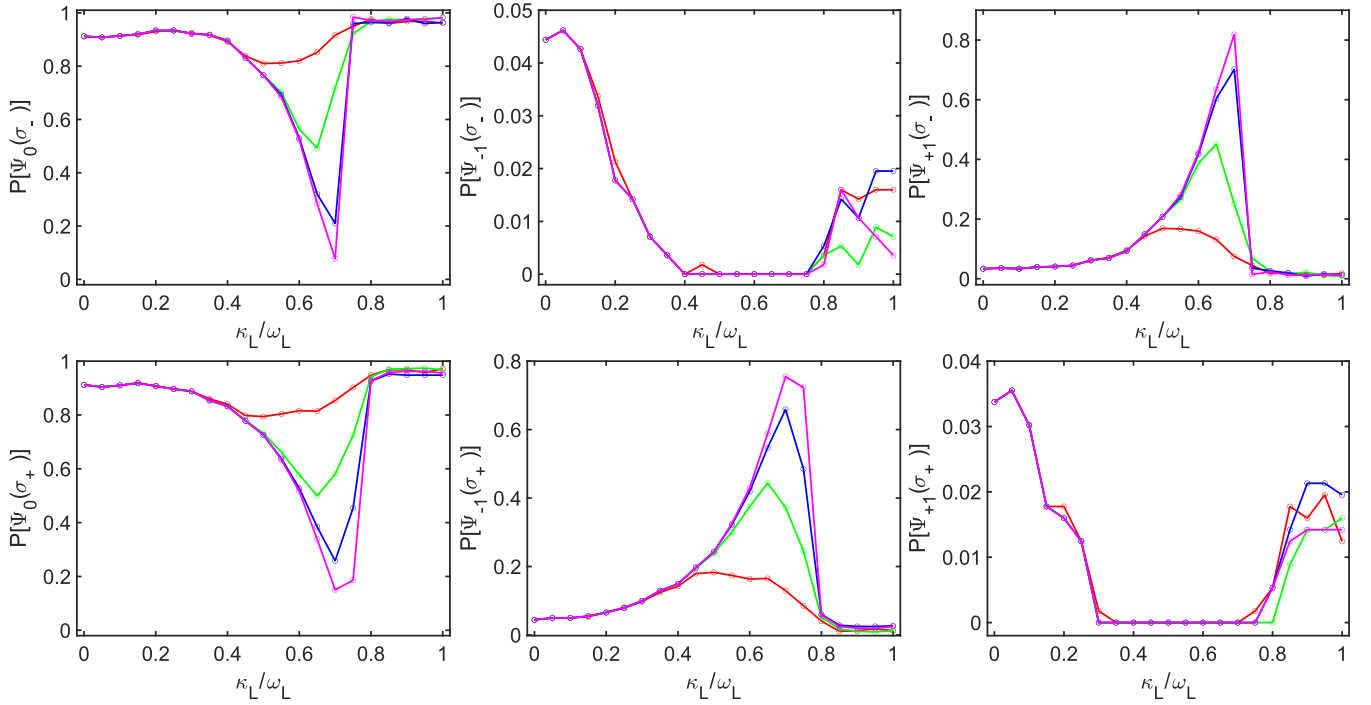


FIG. 3. Probability of a final stationary state  $\psi_n$  as a function of the normalized amplitude  $\kappa_L/\omega_L$  for  $\omega_L = 1.0$ ,  $\delta T = 2$ , and  $\tau_Q^G = 1$ . The upper figures show the case of left circular polarization  $\sigma_-$ , and the lower ones show the case of right circular polarization  $\sigma_+$ . The data are calculated for  $\tau = 25$  (red),  $\tau = 50$  (green),  $\tau = 75$  (blue), and  $\tau = 100$  (magenta). Note the differences in the ordinate scales.

generation as compared to the uniform cooling (up to 20%–30% for the cold spot). The reason for this phenomenon is as follows. As we can see from Eq. (6), the presence of local quench plays the role of an additional force generating harmonics. The leading harmonics in the fluctuation regime is  $n = 0$  and the presence of a local quench of the *cold point* type decreases the effective temperature for  $n = 0$  harmonics. This increases the cooling rate that makes the KZ mechanism of  $|n| = 1$  state generation more efficient. For the *hot point* local quench the situation is inverse, which is why the local quench is less effective for  $|n| = 1$  state formation.

The data presented in (2) show that the initial increase of the probability of  $|n| = 1$  state generation as a function of the local quench parameter is replaced by a decrease for its higher values. This is related to the initial transition into a state strongly localized near a cold point with an optimal size. This specific mode dominates all other types of fluctuations at the critical regime and evolves into an  $n = 0$  state with further slow cooling.

*Effect of circularly polarized light.* We consider the circular polarized electromagnetic wave of frequency  $\omega$  and wave vector  $\mathbf{k}$ , perpendicular to the plane of the ring (right scheme in Fig. 1). The intensity of the radiation is supposed to be weak enough to avoid its heating effect. The electric field for a circularly polarized radiation ( $\sigma_+$  right,  $\sigma_-$  left polarizations) is

$$\mathbf{E}_{\sigma_{\pm}}(\mathbf{r}, t) = E_0[\pm \sin(\mathbf{k} \cdot \mathbf{r} - \omega t), \cos(\mathbf{k} \cdot \mathbf{r} - \omega t), 0], \quad (7)$$

where  $E_0$  is the field amplitude. The corresponding dimensionless angular component of the vector potential is  $A_{\theta}^{\sigma_{\pm}}(\theta, t) = (E_L/\omega_L) \cos(\theta \mp \omega_L t)$ . Here, we introduce the dimensionless frequency  $\omega_L = \omega \tau_{\Delta}$  and the dimensionless field

amplitude  $E_L = E_0 2\pi c \xi_0 / (\Phi_0 \tau_{\Delta}^{-1})$ . Thus the sTDGL equation with the complex relaxation time  $\Gamma_{\Delta} = 1 + i\eta$  acquires the form

$$\begin{aligned} \Gamma_{\Delta} \frac{\partial \psi_n(t)}{\partial t} = & \left[ 1 - \frac{T^G(t) - T_0}{T_{c0} \epsilon_0} - \frac{1}{\epsilon_0 R^2} (n^2) \right] \psi_n(t) \\ & - \Lambda_n^{\sigma_{\pm}} - \sum_{l,m} \{\psi_l(t) \psi_m^*(t)\} \psi_{n+m-l}(t) \\ & - 2 \frac{\kappa_L^2}{\omega_L^2} \psi_n(t) + \zeta_n(t), \end{aligned} \quad (8)$$

where

$$\begin{aligned} \Lambda_n^{\sigma_{\pm}} = & 2 \left( n + \frac{1}{2} \right) \frac{1}{\sqrt{\epsilon_0 R}} \frac{\kappa_L}{\omega_L} e^{-i\omega_L t} \psi_{n\pm 1} \\ & + 2 \left( n - \frac{1}{2} \right) \frac{1}{\sqrt{\epsilon_0 R}} \frac{\kappa_L}{\omega_L} e^{i\omega_L t} \psi_{n\mp 1} \\ & + \frac{\kappa_L^2}{\omega_L^2} e^{-2i\omega_L t} \psi_{n\pm 2} + \frac{\kappa_L^2}{\omega_L^2} e^{2i\omega_L t} \psi_{n\mp 2}, \end{aligned} \quad (9)$$

and  $\kappa_L = E_L / (2\sqrt{\epsilon_0})$ .

Figure 3 demonstrates how the probabilities of the realization of states  $\psi_{n=-1}$ ,  $\psi_{n=0}$ , and  $\psi_{n=+1}$  evolve as a function of the amplitude of the circularly polarized radiation with normalized frequency  $\omega_L = 1.0$ , cooling quench time  $\tau_Q^G = 1$ , and imaginary part of the relaxation constant  $\eta = 0.2$  for several values of the laser pulse duration and for both  $\sigma_-$  and  $\sigma_+$  circular polarizations. The results are obtained at  $t = 200$ , i.e., when the system has reached a stationary regime. Calculations show that only the low harmonics with  $n \leq |1|$  are excited. We may see that in the region, where the role of the circular polar-



ized radiation is important, the positive helicity promotes the  $n = -1$  state realization while it is the  $n = +1$  state, which is promoted for the negative helicity. Importantly, for  $n = |1|$  the ratio of the probabilities of the states  $n = \pm 1$  realization can exceed an order of magnitude. Furthermore the probability of generating the desired current state can be as high as 80%. As we may see from Eq. (8), the term  $2\frac{\kappa_L^2}{\omega_L^2}\psi_n(t)$  plays the role of the increase of temperature and when the condition  $\kappa_L/\omega_L > 1/\sqrt{2}$  is fulfilled, the effective temperature exceeds  $T_{c0}$  and superconductivity may start nucleation only when radiation is switched off.

Our calculations reveal a formation under the influence of the IFE of rather complicated metastable states, involving the higher harmonics  $\psi_n$ . However, when the polarized radiation is switched off, the final states are only  $n = 0$  or  $n = \pm 1$  with the probabilities presented in Fig. 3. (For the individual tracking of stochastic trajectories, see the Supplemental Material [32]).

The IFE is related with the imaginary part of the relaxation constant  $\eta$  and disappears when  $\eta \rightarrow 0$ . The finite value of  $\eta$  is due to the presence of the electron-hole asymmetry [24,27–29], and we may expect relatively large values of  $\eta$  in the multiband superconductors or in superconductors with a not too small  $T_c/E_F$  ratio as the high- $T_c$  superconductors or FeSe superconductors where  $T_c \sim 0.3E_F$  [40].

*Conclusions.* We have demonstrated that a nonhomogeneous thermal quench may strongly increase the probability of spontaneous current generation in small superconducting rings via the KZM. By combining the KZM with the IFE induced by a circular polarized radiation, we may effectively discriminate between the states with different current polarities. Our findings open a way to the all-optical generation of the current states in mesoscopic superconducting systems and allows us to suggest the laser-driven critical dynamics as a method of highly controllable manipulation of the vortex topological charge in superconducting systems.

For the experimental realization of the discussed effects an array of small superconducting rings can be a suitable system. For example, in Ref. [41] the experiments have been performed with Nb nanorings with a width and thickness  $\sim 30\text{--}50$  nm, radius  $R$  as small as 300 nm, and  $\lambda \sim \xi \sim 100$  nm. The nanorings of this type satisfy the conditions of the applicability of our analysis and should generate a magnetic field in an  $n = 1$  current carrying state at the center of the ring of the order of  $B(0) \sim \frac{\Phi_0 \xi^2 \epsilon_0}{\lambda^2 R^2} \sim 10^{-4}T$ . Such a magnetic

field may be easily detected, for example, by a magnetometer based on nitrogen vacancies in a diamond [42–44] or even a nano-SQUID (superconducting quantum interference device) [45].

The sapphire substrate serves as a very effective thermal bath and the thermal quench time is basically determined by the duration of the laser pulse [5,6]. In Ref. [13] the used laser pulse duration was, for example, 2 ps which permitted us to perform the detailed study of the KZM of vortex generation. Such short pulse durations may easily realize a regime with a characteristic dimensionless quench  $\tau_Q^G \sim 1$ , discussed in the present Letter.

Concerning the interplay between KZM and IFE, we note that the dimensionless frequency of the circular polarized radiation  $\omega_L = \frac{\omega\pi\hbar}{8T_{c0}\epsilon_0} \sim 1$  corresponds in the case of Nb to the THz range of the frequencies (or far infrared in the case of the high- $T_c$  superconductors). The intensity of radiation corresponding to the normalized amplitude,  $\kappa_L/\omega_L = \frac{1}{2\sqrt{\epsilon_0}}\frac{E_L}{\omega_L} \approx 0.3$ , where the role of the IFE starts to be pronounced, is  $I_0 \approx 3$  mW/cm<sup>2</sup>. This is a rather modest intensity to provoke a substantial heating of the sample. Indeed, owing to the high thermal conductivity of sapphire [46], which is of the order of 10<sup>3</sup> W/mK, the temperature increase of the superconducting ring on the sapphire substrate of 1  $\mu\text{m}$  thickness will be only of the order of  $3 \times 10^{-2}$  K. Note that the electronic temperature may differ from the lattice (substrate) temperature. In experiments [47] the electron-phonon relaxation time at  $T = 8$  K in thin Nb films was estimated as 0.1 ns. As we consider a quasistationary circular polarized radiation the electron temperature should be basically the same as a lattice one.

*Acknowledgments.* The authors are grateful to A. Melnikov, S. Mironov, J.-B. Trebbia, and V. Plastovets for useful remarks and suggestions. This work was supported by “ANR OPTOFLUXONICS,” the LIGHT S&T Graduate Program (PIA3 Investment for the Future Program, ANR-17-EURE-0027), and GPR LIGHT. M.D.C. acknowledges the University of Bordeaux, the Federal University of Pernambuco Propeq-UFPE program (Edital Propeq No. 05.2018, Recife, Brazil), and the Basic Research Program of the National Research University Higher School of Economics (Moscow, Russia). A.I.B. acknowledges support by the Ministry of Science and Higher Education of the Russian Federation within the framework of state funding for the creation and development of World-Class Research Center (WCRC) “Digital Biodesign and Personalized Healthcare”, Grant No. 075-15-2020-926.

[1] Ya. B. Zeldovich, I. Yu. Kobzarev, and L. B. Okun', Cosmological consequences of a spontaneous breakdown of a discrete symmetry, *Zh. Eksp. Teor. Fiz.* **67**, 3 (1975) [*Sov. Phys. JETP* **40**, 1 (1975)].  
 [2] T. W. B. Kibble, Topology of cosmic domains and strings, *J. Phys.: Math. Gen.* **9**, 1387 (1976).  
 [3] T. W. B. Kibble, Some implications of a cosmological phase transition, *Phys. Rep.* **67**, 183 (1980).  
 [4] W. H. Zurek, Cosmological experiments in superfluid helium?, *Nature (London)* **317**, 505 (1985).

[5] A. Maniv, E. Polturak, and G. Koren, Observation of Magnetic Flux Generated Spontaneously During a Rapid Quench of Superconducting Films, *Phys. Rev. Lett.* **91**, 197001 (2003).  
 [6] D. Golubchik, E. Polturak, and G. Koren, Evidence for Long-Range Correlations within Arrays of Spontaneously Created Magnetic Vortices in a Nb Thin-Film Superconductor, *Phys. Rev. Lett.* **104**, 247002 (2010).  
 [7] D. Golubchik, E. Polturak, G. Koren, B. Y. Shapiro, and I. Shapiro, Experimental determination of correlations between

- spontaneously formed vortices in a superconductor, *J. Low Temp. Phys.* **164**, 74 (2011).
- [8] I. Shapiro, E. Pechenik, and B. Ya. Shapiro, Recovery of superconductivity in a quenched mesoscopic domain, *Phys. Rev. B* **63**, 184520 (2001).
- [9] T. Golod, A. Rydh, and V. M. Krasnov, Detection of the Phase Shift from a Single Abrikosov Vortex, *Phys. Rev. Lett.* **104**, 227003 (2010).
- [10] T. Golod, A. Iovan, and V. M. Krasnov, Single Abrikosov vortices as quantized information bits, *Nat. Commun.* **6**, 8628 (2015).
- [11] S. Mironov, E. Goldobin, D. Koelle, R. Kleiner, P. Tamarat, B. Lounis, and A. Buzdin, Anomalous Josephson effect controlled by an Abrikosov vortex, *Phys. Rev. B* **96**, 214515 (2017).
- [12] J.-Y. Ge, V. N. Gladilin, J. Tempere, J. T. Devreese, and V. V. Moshchalkov, Controlled generation of quantized vortex-antivortex pairs in a superconducting condensate, *Nano Lett.* **17**, 5003 (2017).
- [13] A. Rochet, V. Vadimov, W. Magrini, S. Thakur, J.-B. Trebbia, A. Melnikov, A. I. Buzdin, P. Tamarat, and B. Lounis, On-demand optical generation of single flux quanta, *Nano Lett.* **20**, 6488 (2020).
- [14] R. Monaco, J. Mygind, R. J. Rivers, and V. P. Koshelets, Spontaneous fluxoid formation in superconducting loops, *Phys. Rev. B* **80**, 180501(R) (2009).
- [15] J. R. Kirtley, C. C. Tsuei, and F. Tafuri, Thermally Activated Spontaneous Fluxoid Formation in Superconducting Thin Film Rings, *Phys. Rev. Lett.* **90**, 257001 (2003).
- [16] S. Mironov, A. S. Mel'nikov, I. D. Tokman, V. Vadimov, B. Lounis, and A. Buzdin, Inverse Faraday Effect for Superconducting Condensates, *Phys. Rev. Lett.* **126**, 137002 (2021).
- [17] A. Kirilyuk, A. V. Kimel, and T. Rasing, Laser-induced magnetization dynamics and reversal in ferrimagnetic alloys, *Rep. Prog. Phys.* **76**, 026501 (2013).
- [18] A. Kirilyuk, A. V. Kimel, and T. Rasing, Ultrafast optical manipulation of magnetic order, *Rev. Mod. Phys.* **82**, 2731 (2010).
- [19] C. Ryu, M. F. Andersen, P. Cladé, V. Natarajan, K. Helmerson, and W. D. Phillips, Observation of Persistent Flow of a Bose-Einstein Condensate in a Toroidal Trap, *Phys. Rev. Lett.* **99**, 260401 (2007).
- [20] S. Beattie, S. Moulder, R. J. Fletcher, and Z. Hadzibabic, Persistent Currents in Spinor Condensates, *Phys. Rev. Lett.* **110**, 025301 (2013).
- [21] M. Lu-Dac and V. V. Kabanov, Multiple phase slips phenomena in mesoscopic superconducting rings, *Phys. Rev. B* **79**, 184521 (2009).
- [22] R. Rounds, B. Sarkar, D. Alden, Q. Guo, A. Klump, C. Hartmann, T. Nagashima, R. Kirste, A. Franke, M. Bickermann, Y. Kumagai, Z. Sitar, and R. Collazo, The influence of point defects on the thermal conductivity of AlN crystals, *J. Appl. Phys.* **123**, 185107 (2018).
- [23] A. Abdullaev, V. S. Chauhan, B. Muminov, J. O'Connell, V. A. Skuratov, M. Khafizov, and Z. N. Utegulov, Thermal transport across nanoscale damage profile in sapphire irradiated by swift heavy ions, *J. Appl. Phys.* **127**, 035108 (2020).
- [24] N. B. Kopnin, *Theory of Nonequilibrium Superconductivity* (Clarendon Press, Oxford, U.K., 2001).
- [25] L. P. Gor'kov and N. B. Kopnin, Vortex motion and resistivity of type-II superconductors in a magnetic field, *Usp. Fiz. Nauk* **116**, 413 (1975); [*Sov. Phys. Usp.* **18**, 496 (1975)].
- [26] B. I. Ivlev and N. B. Kopnin, Theory of current states in narrow superconducting channels, *Usp. Fiz. Nauk* **142**, 435 (1984); [*Sov. Phys. Usp.* **27**, 206 (1984)].
- [27] N. B. Kopnin, B. I. Ivlev, and V. A. Kalatsky, Sign reversal of the flux-flow Hall effect in type-II superconductors, *Pisma Zh. Eksp. Teor. Fiz.* **55**, 717 (1992) [*JETP Lett.* **55**, 750 (1992)].
- [28] A. T. Dorsey, Vortex motion and the Hall effect in type-II superconductors: A time-dependent Ginzburg-Landau theory approach, *Phys. Rev. B* **46**, 8376 (1992).
- [29] A. I. Larkin and A. A. Varlamov, in *Physics of Conventional and Nonconventional Superconductors*, edited by K.-H. Bennemann and J. B. Ketterson (Springer, Berlin, 2002).
- [30] C. W. Gardiner, *Handbook of Stochastic Methods for Physics, Chemistry and the Natural Science* (Springer, Berlin, 2003).
- [31] N. G. Van Kampen, *Stochastic Processes in Physics and Chemistry* (Elsevier/North-Holland, Amsterdam, 2007).
- [32] See Supplemental Material at <http://link.aps.org/supplemental/10.1103/PhysRevB.105.L020504> for more details, such as derivation of the dimensionless stochastic force term as well as individual tracking of stochastic trajectories.
- [33] D. E. McCumber and B. I. Halperin, Time scale of intrinsic resistive fluctuations in thin superconducting wires, *Phys. Rev. B* **1**, 1054 (1970).
- [34] A. Schmid, Diamagnetic Susceptibility at the Transition to the Superconducting State, *Phys. Rev.* **180**, 527 (1969).
- [35] J. Berger, Ginzburg-Landau equations with consistent Langevin terms for nonuniform wires, *Phys. Rev. B* **75**, 184522 (2007).
- [36] R. G. McDonald and A. S. Bradley, Reservoir interactions during Bose-Einstein condensation: Modified critical scaling in the Kibble-Zurek mechanism of defect formation, *Phys. Rev. A* **92**, 033616 (2015).
- [37] S. Hannibal, P. Kettmann, M. D. Croitoru, V. M. Axt, and T. Kuhn, Dynamical vanishing of the order parameter in a confined Bardeen-Cooper-Schrieffer Fermi gas after an interaction quench, *Phys. Rev. A* **97**, 013619 (2018).
- [38] S. Hannibal, P. Kettmann, M. D. Croitoru, V. M. Axt, and T. Kuhn, Persistent oscillations of the order parameter and interaction quench phase diagram for a confined Bardeen-Cooper-Schrieffer Fermi gas, *Phys. Rev. A* **98**, 053605 (2018).
- [39] J. Dziarmaga, P. Laguna, and W. H. Zurek, Symmetry Breaking with a Slant: Topological Defects after an Inhomogeneous Quench, *Phys. Rev. Lett.* **82**, 4749 (1999).
- [40] S. Kasahara, T. Watashige, T. Hanaguri, Y. Kohsaka, T. Yamashita, Y. Shimoyama, Y. Mizukami, R. Endo, H. Ikeda, K. Aoyama, T. Terashima, S. Uji, Th. Wolf, H. von Löhneysen, T. Shibauchi, and Y. Matsuda, Field-induced superconducting phase of FeSe in the BCS-BEC cross-over, *Proc. Natl. Acad. Sci. USA* **111**, 16309 (2014).
- [41] O. J. Sharon, A. Shaulov, J. Berger, A. Sharoni, and Y. Yeshurun, Current-induced SQUID behavior of superconducting Nb nano-rings, *Sci. Rep.* **6**, 28320 (2016).
- [42] L. Thiel, D. Rohner, M. Ganzhorn, P. Appel, E. Neu, B. Müller, R. Kleiner, D. Koelle, and P. Maletinsky, Quantitative nanoscale vortex imaging using a cryogenic quantum magnetometer, *Nat. Nanotechnol.* **11**, 677 (2016).
- [43] T. Lenz, A. Wickenbrock, F. Jelezko, G. Balasubramanian, and D. Budker, Magnetic sensing at zero field with a single nitrogen-vacancy center, *Quantum Sci. Technol.* **6**, 034006 (2021).

- [44] D. Paone, D. Pinto, G. Kim, L. Feng, M.-J. Kim, R. Stöhr, A. Singha, S. Kaiser, G. Logvenov, B. Keimer, J. Wrachtrup, and K. Kern, All-optical and microwave-free detection of Meissner screening using nitrogen-vacancy centers in diamond, *J. Appl. Phys.* **129**, 024306 (2021);
- [45] J. R. Kirtley, L. Paulius, A. J. Rosenberg, J. C. Palmstrom, C. M. Holland, E. M. Spanton, D. Schiessl, C. L. Jermain, J. Gibbons, Y.-K.-K. Fung, M. E. Huber, D. C. Ralph, M. B. Ketchen, G. W. Gibson, Jr., and K. A. Moler, Scanning SQUID susceptometers with sub-micron spatial resolution, *Rev. Sci. Instrum.* **87**, 093702 (2016).
- [46] R. Berman, E. L. Foster, and J. M. Ziman, Thermal conduction in artificial sapphire crystals at low temperatures I. Nearly perfect crystals, *Proc. R. Soc. London, Ser. A* **231**, 130 (1955).
- [47] E. M. Gershenson, M. E. Gershenson, G. N. Gol'tsman, M. Lyul'kin, A. D. Semenov, and A. V. Sergeev, Electron-phonon interaction in ultrathin Nb films, *Zh. Eksp. Teor. Fiz.* **97**, 901 (1990) [*Sov. Phys. JETP* **70**, 505 (1990)].